Enhanced Pedestal Pressure and Parameter-Linkages Determining Edge Pedestal Structure in JT-60U Type I and Type II ELMy H-mode

Y. Kamada 1), H. Takenaga 1), H. Urano 2), T. Takizuka 1), T. Hatae 1) ,Y. Miura 1)

1) Japan Atomic Energy Research Institute, Naka Fusion Research Establishment, Ibaraki-ken, Japan
2) Max-Planck-Institut fur Plasmaphysik, Garching, Germany

e-mail contact of main author: kamada@naka.jaeri.go.jp

Abstract. Based on the expanded H-mode operational regimes in JT-60U utilizing the improved capability of high triangularity (δ) operation, the multiple pellet injection and high power heating including the negative ion based NB (NNB), we have clarified the pedestal parameter-linkages determining the pedestal structure (i.e. 'The pedestal width' increases with ρ_{pi} and does not depend on $\beta_{p\text{-}ped}$. 'The normalized pressure gradient α' is almost constant at low δ, while $\alpha \propto \beta_p$ at high δ). Based on these results, we have enhanced the pedestal pressure of the ELMy H-mode by factors of 2-2.5 at the same plasma current and plasma shape, and extended the high confinement regime to a high density. We have found that the pedestal stored energy W_{ped} increases with the core energy (or β_p-core) at high δ (>0.3-0.4), while W_{ped} is low and almost constant independent of, for example, heating power at low δ (<0.2). In addition, we have expanded the type II (grassy) ELMy high confinement regime with a small heat load on to divertor plates to the low-q (q_{95}<4) regime, and demonstrated successful compatibility of the type II ELMs with the pellet injection. Based on a variety of JT-60U experiments, possible linkages among the pedestal and the core parameters has been proposed.

1. Introduction

The H-mode edge pedestal condition determines the burning plasma performances, such as the fusion gain, since it determines the core confinement as the boundary condition and affects the stable β limit through the global current and pressure profiles. Therefore, study on the pedestal structure and its response to external controls has been raised as one of the urgent research subjects in the world tokamak research activities [1-4]. The pedestal structure [5] is determined by 1) formation and dynamics of the transport barrier [6-8] governed by transport bifurcations [9,10] and 2) by appearance of the edge localized modes (ELMs) [11,12]. Based on these physics understandings, we need a global treatment of transport [9,13] and stability [12] characteristics including core, pedestal, and SOL regions in order to expand the H-mode operational regimes [14] towards the high integrated fusion performance [15] in ITER and DEMO reactors. From this point of view, JT-60U has devoted large efforts on understandings of the edge pedestal and expanded the operational regimes of the ELMy H-mode [16]. This paper reports recent results of JT-60U contributing to the two urgent research subjects; extension of the high confinement regime to high density, and expansion of the small (Type II) ELM regime towards low q_{95}. In addition, based on a variety of JT-60U experiments, we propose possible linkages among the pedestal and the core parameters.

2. Density Regime Extended by Enhanced Pedestal Pressure

We applied multiple pellet injection into the high-β_p ELMy H-mode discharges and the high confinement regime was extended to n_e/n_{GW} ~0.7 (Fig.1(a)) [17]. In these cases, the pellets penetrated just inside the pedestal width Δ_{ped} and the electron density n_e was increased gradually (~$20\tau_E$) so as not to decrease the pedestal temperature (since Δ_{ped} increases with the thermal ion poloidal gyro radius ρ_{pi} as described below). In addition, we increased β_p above 2 with an optimum heating profile consisting of the positive and negative ion source NBs to keep MHD stability. Consequently, we have enhanced W_{ped} by factors of 2-2.5 for the type I ELMy edge at the same plasma current and plasma shape (I_p=1MA, δ=0.44-0.5; Figs.1(b),(c) and 2) , and achieved H_{89PL}=2.1 (H_{Hy2}=1.1) at n_e=0.7n_{GW}. At the same density, $H_{89PL}$was 1.3 in the gas-fuelled reference cases. Figure 1(b) and (c) compares time evolution of the representative discharges with pellet injection and gas fueling, respectively. Figure 2(a) shows that the pedestal ion temperature is high (by a factor of 2.5) and Δ_{ped} is wide in the pellet injection case compared with gas fueling at the same pedestal density. Figure 2(b) (treating discharges at 1MA and δ=0.44-0.50) shows that the pedestal pressure (p_e^{PED}= n_e^{PED}xT_e^{PED}) stays roughly constant for the standard ELMy H-mode with type I ELMs (open circles). While in the high β_p ELMy H-mode

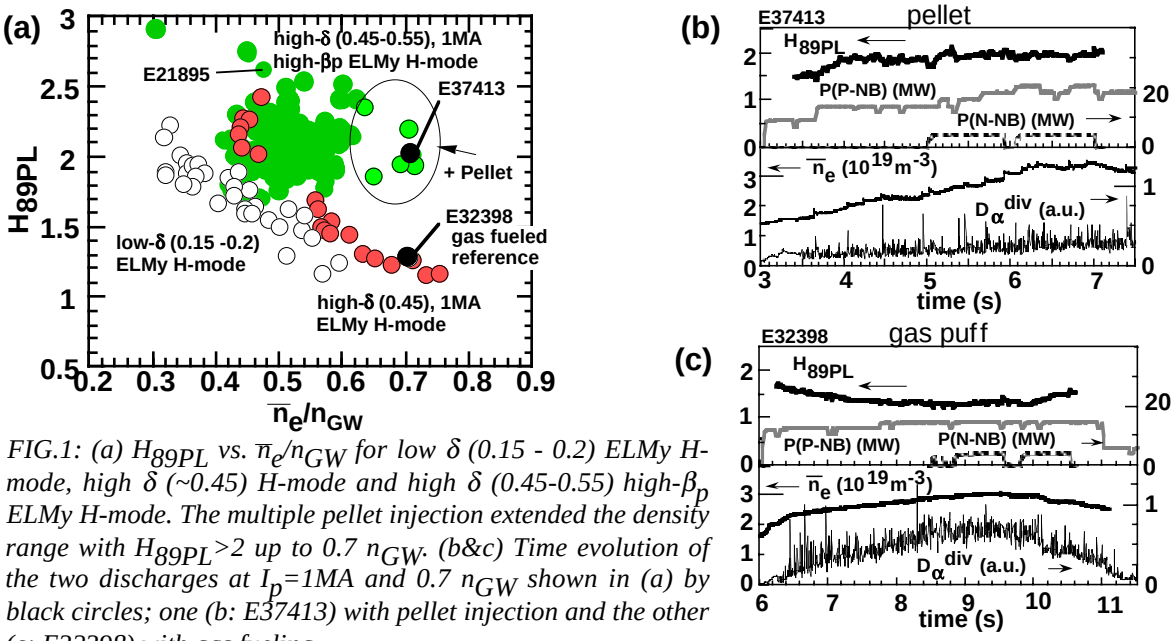

FIG.1: (a) H_{89PL} vs. $\bar{n}_e/n_{GW}$ for low δ (0.15 - 0.2) ELMy H-mode, high δ (~0.45) H-mode and high δ (0.45-0.55) high-β_p ELMy H-mode. The multiple pellet injection extended the density range with H_{89PL}>2 up to 0.7 n_{GW}. (b&c) Time evolution of the two discharges at I_p=1MA and 0.7 n_{GW} shown in (a) by black circles; one (b: E37413) with pellet injection and the other (c: E32398) with gas fueling.

(closed circles), p_e^{PED} can be higher. In the pellet injected cases, p_e^{PED} increases gradually (see the time evolution of E37413), and reaches high values. On the other hand, in the gas-fueled case (E32398), T_e^{PED} decreases with increasing n_e^{PED}. The pedestal temperature in E37413 is higher than that in E32398 by a factor of 2.3. We have also achieved high pedestal pressure with the type II ELMs (crosses in Fig.2(b)). Such type II ELMs were obtained without pellet injection and in the relatively high T_e^{PED} regime as shown in Fig.2(b).

3. Pedestal Structure

Figure 3 shows dependence of the pedestal parameters on the total β_p values (β_p-tot). Figure 3(a) shows the pedestal β_p (β_p-ped) increases with β_p-tot at high δ ~0.44 -0.50. This relationship appears independent of existence of the ITB, which means that this relation does not come from the profile stiffness. On the other hand, β_p-ped is almost constant at low δ.

The pedestal pressure is sustained by both the width Δ_{ped} and the gradient ∇p. Figure 3(b) shows that Δ_{ped} is independent of β_p-tot (and also β_p-ped, since β_p-tot ∝ β_p-ped as shown in Fig.3(a)). Figure 3(c) shows that the pedestal width follows the scaling Δ_{ped}~$5\rho_{pi}q_{95}^{0.3}$ [18]. Previously, β_p-ped and ρ_{pi} had a strong correlation experimentally. However, recently, the pellet injection and the NNB injection

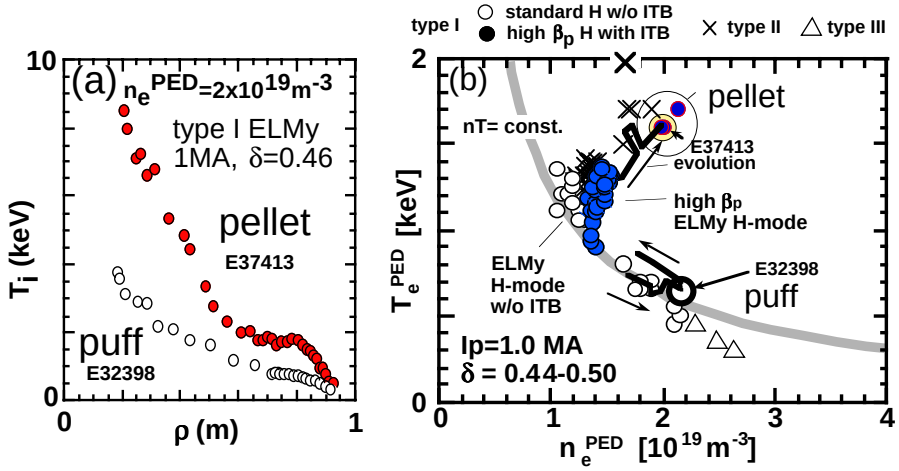

FIG.2: (a) Ion temperature profiles for pellet and gas fueled type I ELMy H-mode discharges at the same n_e^{PED} (I_p=1MA, δ=0.46). (b) Pedestal electron temperature T_e^{PED} vs. density n_e^{PED} at I_p=1MA and δ=0.44-0.50.

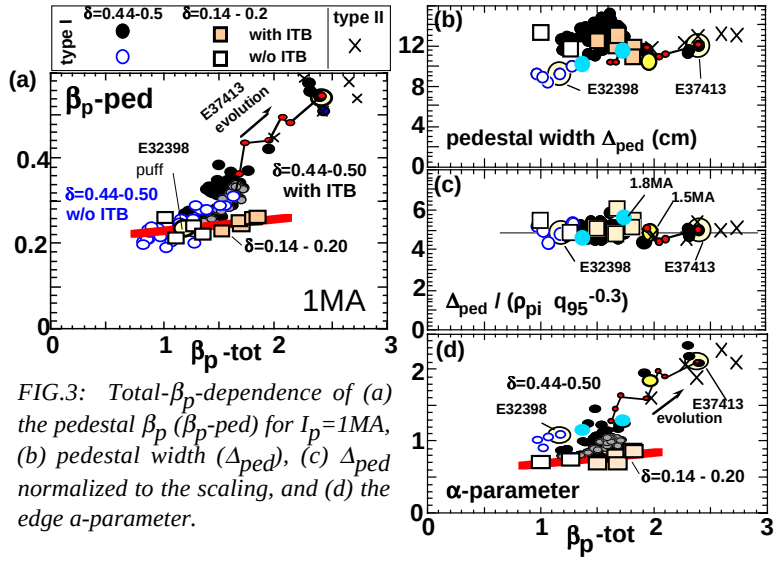

FIG.3: Total-β_p-dependence of (a) the pedestal β_p (β_p-ped) for I_p=1MA, (b) pedestal width (Δ_{ped}), (c) Δ_{ped} normalized to the scaling, and (d) the edge a-parameter.

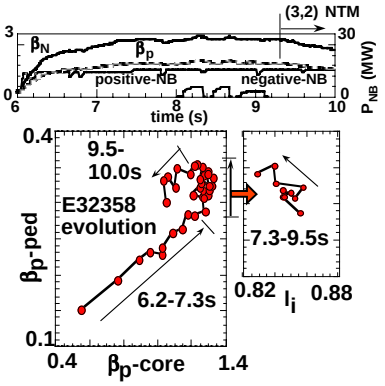

FIG.4: Evolution of the high-β_p type I ELMy discharge (δ=0.46, 1MA). At first, β_p-ped increases with β_p-core (6.2-7.3s). Then, β_p-ped increases with l_i during the phase when β_p-core was almost saturated (7.3-9.5s).

enabled these two parameters to be decoupled.

Figure 3(d) shows that, at high δ (circles), the normalized pressure gradient, the α-parameter, increases with β_p-tot. On the other hand, at low δ (squares), it is almost constant at a low value. This β_p-dependence may be due to increasing Shafranov shift [19] or radially increasing filed line pitch at the low field side.

Figure 4 shows time evolution of the high-δ high β_p type I ELMy H-mode discharge E32358. In this discharge, β_p-ped increases with β_p-core, and after saturation of β_p-core, β_p-ped increases gradually with decreasing l_i with a slow time constant of ~2 sec (~$10\tau_E$) which is comparable with the edge current diffusion time over the pedestal layer.

In Fig.3, the type II ELM data follow the similar dependence. Based on these observation, the pressure gradient of the type I and type II ELMy edge is determined by δ, β_p-tot (or β_p-core) and the edge current driven mainly by the bootstrap current.

4. Pedestal Stored Energy and Parameter-Linkages

The dependence of β_p-ped on β_p-tot was different between low and high δ discharges as shown in Fig.3(a). In order to clarify the δ-dependence of the pedestal stored energy W_{ped}, Fig.5 shows W_{ped} normalized by the pedestal term of the offset-nonlinear scaling proposed in ref.[20] (W_{ped}^{ONL}~κRa$I_p B_t$) at a fixed q_{95} (=3.0 – 3.8). We have found that upper boundary of W_{ped} increases with δ (Fig.5(a)), and that W_{ped} increases with the core energy at high δ (Fig.5(b)). In the previous scalings of W_{ped} [3,20,21], W_{ped} for the type I ELMy H-mode was expressed as P_{ped}(~W_{ped}/V) ~ $B^2 f$(shape), where V is the plasma volume, B is the magnetic field (combination of B_t and I_p/a), and *f* is the function of the plasma shape.

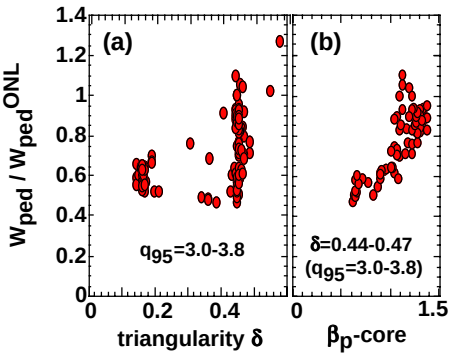

FIG.5: Pedestal stored energy normalized to the pedestal term of the Offset-nonlinear scaling: dependence on triangularity and β_p-core .

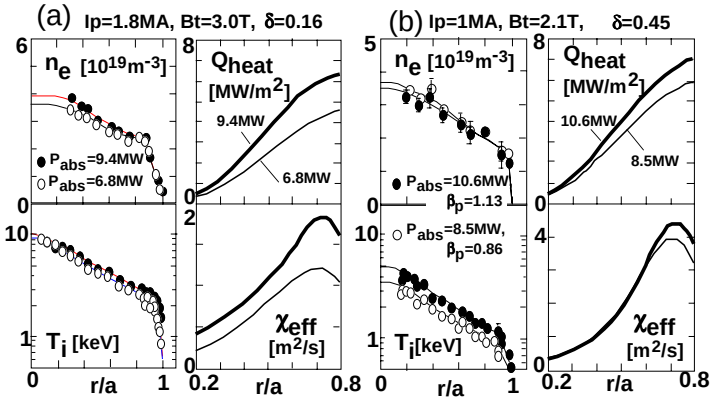

FIG.6: Comparison of the profiles of electron density n_e, ion temperature T_i, heat flux Q_{heat}, and effective heat diffusivity χ_{eff} at two different heating power for (a) the low δ (=0.16) and (b) the high δ (=0.45) configurations.

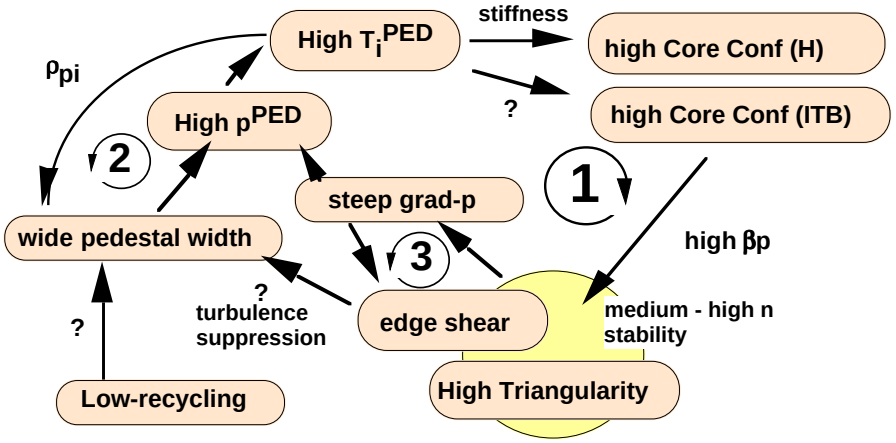

FIG.7: Possible correlations (feedback loops) among pedestal and core parameters: Loop (1) ; Improved pedestal stability (high δ, high β_p, magnetic shear) steepens pedestal pressure gradient and enhances pedestal pressure (p^{PED}). High p^{PED} allows high pedestal temperature (T^{PED}). High T^{PED} improves core confinement when core kinetic profile shapes are stiff. High core confinement increases β_p. Loop (2); High T^{PED} widens pedestal width and then enhances p^{PED}. Loop (3); Pedestal pressure gradient drives bootstrap current and affects edge magnetic shear.

It should be noted that this expression is independent of the heating power. This power-independence holds at low δ (<0.2) in JT-60U. (As shown in Fig.3(a), β_p-ped is almost constant and independent of β_p-tot). On the other hand, at high-δ, W_{ped} increases with β_p-core. This result means that W_{ped} increases with heating power at high-δ. Accordingly, we conclude that the pedestal term of the confinement scaling law should be a non linear function on δ depending on $\beta_p(\delta)$.

The degradation of the H-mode confinement at high density is explained that T^{PED} decreases with increasing n_e^{PED} because p^{PED} is constant, and temperature in the core region decreases in proportion to decreasing T^{PED} due to appearance of the profile stiffness [22]. Figure 6 shows that the scale length of T_i is almost constant and independent of the heating power for both low-δ (Fig.6(a)) and high-δ (Fig.6(b))[23]. However, at high-δ, T_i^{PED} becomes high at high heating power P_{abs}, while T_i^{PED} is almost unchanged at low-δ. Consequently, χ_{eff} in the core region increases largely with increasing P_{abs} at low-δ.

Figure 7 summarizes possible correlations among pedestal and core parameters based on the observations in JT-60U. In order to achieve a steep pedestal pressure gradient, high δ, high β_p and edge magnetic shear control are required [24-27]. Effects of the edge magnetic shear on the edge turbulence suppression (thus on the pedestal width) [28] has not been clarified in JT-60U. The steep ∇p enhances pedestal pressure. The high pedestal pressure allows a high pedestal temperature at a given pedestal density. The high pedestal temperature widens the pedestal width (ρ_{pi} dependence [18,29]). The wide

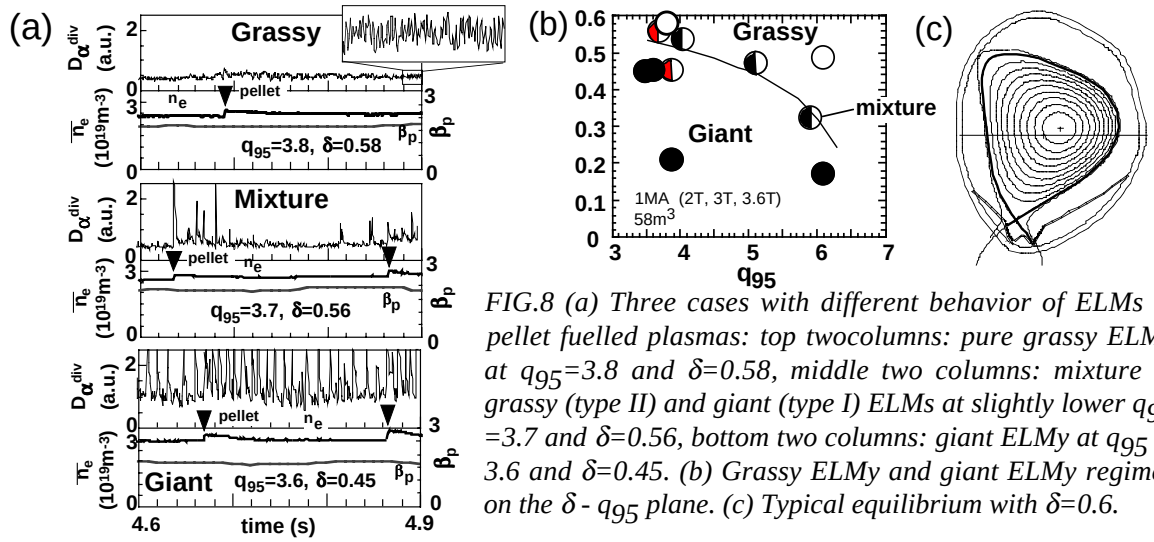

FIG.8 (a) Three cases with different behavior of ELMs in pellet fuelled plasmas: top twocolumns: pure grassy ELMy at q_{95}=3.8 and δ=0.58, middle two columns: mixture of grassy (type II) and giant (type I) ELMs at slightly lower q_{95} =3.7 and δ=0.56, bottom two columns: giant ELMy at q_{95} = 3.6 and δ=0.45. (b) Grassy ELMy and giant ELMy regimes on the δ - q_{95} plane. (c) Typical equilibrium with δ=0.6.

pedestal width enhances the pedestal pressure and the pedestal temperature. High pedestal temperature improves the core confinement for the standard ELMy H-mode [22,23,30]. It has not been clarified that the high edge temperature helps the ITB formation. However, at least for the high β_p mode, high-δ plasmas seem to have relatively lower threshold heating power for ITB formation with a clear electron temperature internal barrier [31]. And then, if the core confinement (or β_p) is improved, the pedestal stability is improved. According to Fig.4 and ref.[18], the time constant required for this positive feedback cycle (loop '1' in Fig.7) seems to be ~2sec ($10\tau_E$) at I_p=1MA. Therefore, when we increase density, we need to fit the rise time to this time scale. In practice, in the pellet injected discharge E37413 (Figs.1-3), the slow density rise over 3sec was successful. On the other hand, a strong gas puff decreases the pedestal temperature which may force the plasma to follow the negative feedback loop.

5. Extension of the type II ELM regime to q_{95}<4

The type II ELM appears at high-δ and high-q_{95} [17,24,25,32]. The high δ operation capability extended recently in JT-60U enables δ=0.6 at I_p=1MA. With δ=0.58, we have sustained the type II ELMy H-mode at q_{95}=3.8 (Fig.8), and expanded the operational regime having high confinement with an ITB (H_{Hy2}>1.1), high β_N>2.8 and small peak heat load (~1/5 of the type I ELMs) to this low-q_{95} regime. In addition, we demonstrated favorable compatibility of the type II ELMs with pellet injection (Fig.8(a)) when the pellet penetration is deeper than the pedestal width. At a smaller δ or q_{95}, type I ELMs appear after each pellet. At a medium δ (~0.45), type I ELMs governs the discharges.

Acknowledgments
The authors would like to thank the JT-60 Team and the members of the ITPA Edge & Pedestal Group.

REFERENCES

[1] the task definition and the annual report of the Edge and Pedestal Physics Topical Group in the International Tokamak Physics Activity (ITPA), http://itpa.ipp.mpg.de.
[2] Hatae, T., et al., Nucl., Fusion **41**, 285 (2001)
[3] Horton, L.D., et al, Plasma Phys. Control. Fusion **44** (2002) A273
[4] Osborne, T. H., et al., this conference IAEA-CN-94 / CT-3.
[5] Hubbard, A. E., Plasma Phys. Control. Fusion **42** (2000) A15.
[6] Kamada, Y., Plasma Phys. Control. Fusion **42** (2000) A65.
[7] Fujita, T., Plasma Phys. Control. Fusion **44** (2002) A19.
[8] Gohil, P., Plasma Phys. Control. Fusion **44** (2002) A37.
[9] Parail, V.V. , Plasma Phys. Control. Fusion **44** (2002) A63.
[10] Hahm, T. S. , Plasma Phys. Control. Fusion **44** (2002) A87.
[11] Suttrop, W. , Plasma Phys. Control. Fusion **42** (2000) A1.
[12] Lao, L.L. , Plasma Phys. Control. Fusion **42** (2000) A51.
[13] Janeschiz, G., et al., Plasma Phys. Control. Fusion **44** (2002) A459.
[14] Horton, L.D., Plasma Phys. Control. Fusion **42** (2000) A37.
[15] Kamada Y., et al., Nucl. Fusion **41** (2001) 1311.
[16] Kamada Y., et al., Fusion Science and Technology **42** (2002) 185.
[17] Kamada Y, et al., Plasma Phys. Control. Fusion **44** (2002) A279.
[18] Kamada Y, et al., Plasma Phys. Control. Fusion **41** (1999) 1371.
[19] W.H. Choe and J.P.Freidberg, Phys. Fluids **29** (1986) 1766.
[20] Takizuka, T, Plasma Phys. Control. Fusion **40** (1998) 851.
[21] Thomsen, K., et al., Plasma Phys. Control. Fusion **44** (2002) A429.
[22] Urano, H., et al., Nucl. Fusion **42** (2002) 76.
[23] Urano, H., et al., Plasma Phys. Control. Fusion **44** (2002) A437.
[24] Kamada, Y., et al., Plasma Phys. Control. Fusion 38 (1996) 1387.
[25] Kamada, Y., et al., Plasma Phys. Control. Nucl. Fusion Res., Proc 16th Int. Conf. (Montreal, 1996) Vol.1 (Vienna: IAEA) p247.
[26] Lao, L. L., et al., Nucl. Fusion **41** (2002) 295.
[27] Oyama, N., et al., Plasma Phys. Control. Fusion **43** (2001) 717.
[28] Sugihara M., et al., Plasma Phys. Control. Fusion **44** (2002) A299.
[29] Hatae,T., et al., Plasma Phys. Control. Fusion **40** (1998) 1073.
[30] Kubo, H., et al., Nucl. Fusion **41** (2001) 227.
[31] Kamada, Y., et al., Nucl. Fusion **39** (1999) 1845.
[32] Kamada,Y.,etal., Plasma Phys. Control. Fusion **42** (2000) A247.